Biogeochemistry (2006) 78: 315–342
DOI 10.1007/s10533-005-4426-6


# Experimental test of a mechanistic model of production, flux and gas bubble zonation in non-vegetated flooded rice field soil

ANDRE KUSMIN[1,2], NIKOLAI M. BAZHIN[3] and RALF CONRAD[1,*]
*[1]Max-Planck-Institut für terrestrische Mikrobiologie, Karl-von-Frisch-Str., 35043 Marburg, Germany; [2]Present address: Institute of Chemistry, Free University of Berlin, Takustr. 3, 14195 Berlin, Germany; [3]Institute of Chemical Kinetics and Combustion, Institutskaya 3, Novosibirsk 630090, Russia; *Author for correspondence (e-mail: Conrad@staff.uni-marburg.de; phone: +49-6421-178801; fax: +49-6421-178809)*

Received 1 March 2005; accepted in revised form 24 October 2005

**Key words:** Concentration gradient, Diffusive flux model, Ebullition, Methane production, Rice field soil

**Abstract.** Anoxic wetlands are an important source for the greenhouse gas $CH_4$, much of which is emitted in form of gas bubbles. The conditions for formation of gas bubbles have recently been described by an analytical model, which allows the prediction of fluxes by first physical principles using the knowledge of gas concentration profiles and/or gas production rates. We tested parts of this model by experiments using microcosms of flooded, non-vegetated and homogeneous rice field soil incubated under different gas atmospheres and at different temperatures. In these experiments we determined rates of $CH_4$ and $CO_2$ production, upper boundaries of the bubble zone, gas-filled porosities and vertical profiles of dissolved $CH_4$, $CO_2$ and $N_2$. The results of our experiments confirmed that by knowing only one of the following parameters, i.e. $CH_4$ production, diffusive $CH_4$ flux and depth of upper boundary of bubble zone, the remainder could be predicted from the model. On average, predicted values differed from experimental ones by a factor of 0.4 –2.7, depending on which parameter was taken as an input for the model. It was possible to predict the percentage of gas bubble flux from measured $CH_4$ emission rates under the experimental conditions, which was on the order of 90%. The confrontation of the model with experimental data showed that the effect of the shallow upper oxic layer on bubble formation was negligible and that the $CH_4$ diffusive flux is easily underestimated by experiments lacking sufficient spatial resolution. Therefore, $CH_4$ production rates lower than in our microcosms would allow a more precise test of the model by creating less steep concentration gradients, which, however, would require long incubation times to purge the dissolved $N_2$ from the soil by ebullition and to reach true steady state.

## List of symbols

$i$ – subscript denoting either of $CH_4$, $CO_2$, $O_2$, $N_2$ or He.
ã – thickness of a upper layer, where all forming $CH_4$ would escape through molecular diffusion only. See Bazhin (2003)
$A$ – gas concentration gradient at the surface ($z = 0$) of soil layer (mole $cm^{-4}$)
$b_0$ – thickness of water column which provides pressure of 1 atm.
$b$ – thickness of water column above the soil layer

$B$ – coefficient originating from boundary conditions (mole $cm^{-3}$)

$B_1$, $B_2$ – coefficients resulting from the fit of equation $y = B_2z + B_1$ to a concentration profile

$C_{water}$ – dissolved gas concentration (mole $cm^{-3}$ of aqueous phase)

$C$, $C_{soil}$ – dissolved gas concentration (mole $cm^{-3}$ of flooded soil)

$D_{water}$ – gas diffusion coefficient in water ($cm^2$ $s^{-1}$)

$D$, $D_{soil}$ – gas diffusion coefficient in the flooded soil ($cm^2$ $s^{-1}$)

$E$ – gas emission rates (mole $s^{-1}$)

$h$ – the upper boundary of bubble formation (cm)

$K_{water}$ – Henry's constant for water (mole $cm^{-3}$ $bar^{-1}$)

$K$, $K_{soil}$ – Henry's constant for the flooded soil (mole $cm^{-3}$ of flooded soil $bar^{-1}$)

$l$ – characteristic length for the flooded soil microcosm (cm)

$P_0$ – atmospheric pressure (bar)

$P$ – partial pressure (bar) of a gas in the atmosphere

$P_{dry}$ – gas production rates per gram of dry soil (mole $g^{-1}$ $s^{-1}$)

$S$ – surface area of the microcosm ($cm^2$)

$V_{flooded}$ – total volume of flooded soil ($cm^3$)

$V_{bubbles}$ – total volume occupied by bubbles ($cm^3$)

$W$ – gas production rate (mole $cm^{-3}$ of flooded soil $s^{-1}$)

$W^{I}$, $W^{II}$ – gas production rates in the Region I and II, respectively

$W_{CO_2\text{-ox}}$ – $CO_2$ production rate (due to aerobic processes) in the oxic layer

$x$ – thickness of upper oxic layer (cm)

$X$ – gas mixing ratio in the atmosphere above the microcosm

$z$ – depth coordinate, unless specified (cm)

$\varphi_w$ – experimentally determined actual water-filled porosity

$\varphi_w^I$ – experimentally determined water-filled porosity of bubble-free soil, $\varphi_w^I = \Delta M/(V_{flooded} - V_{bubbles})$

$\varphi_g$ – gas-filled porosity

$\gamma$ – saturation parameter ($cm^{-1}$)

## Introduction

Methane production is the dominant terminal process for organic matter decomposition in anoxic environments (swamps, marshes, fens, lakes, rice paddies). It takes place if oxygen and alternate inorganic electron acceptors such as nitrate, ferric iron or sulfate are not available (Zehnder and Stumm 1988). Methane is a greenhouse gas and contributes significantly to global warming (Watson et al. 1992). The atmospheric abundance of $CH_4$ has been

increasing by 0.45% per year (Lelieveld et al. 1998; Wang et al. 2004). Particularly, rice paddies and natural wetlands are among the dominant sources of atmospheric $CH_4$ contributing, about 20–50% to the total budget (Lelieveld et al. 1998; Wang et al. 2004).

Methane emission from wetland soils is mostly controlled by production, oxidation and transport of $CH_4$ from the soil into the atmosphere. There are three main mechanisms of methane emission: transport by plants, molecular diffusion and ebullition (Conrad 1989). In vegetated wetlands, plant-mediated transport is the most important pathway accounting for up to 90% of total $CH_4$ emission (Schütz et al. 1991; Chanton and Dacey 1991; Grosse et al. 1996). However, ebullition can also be important. For example, it may account for 40–90% of total $CH_4$ flux in hypertrophic freshwater lakes (Keller and Stallard 1994; Chanton and Whiting 1995; Casper et al. 2000), peat bogs (Lansdown et al. 1992) and sometimes also in rice fields (Chareonsilp et al. 2000; Wassmann et al. 1996). Methane emission by molecular diffusion through the soil and water layers usually is not important, since methanotrophic bacteria oxidize 80–100% of the $CH_4$ passing through the oxic zones at the surface (Frenzel et al. 1990; Conrad and Rothfuss 1991). Transport through plants also results in attenuation of the $CH_4$ flux because of microbial oxidation in the rhizosphere, accounting for a reduction in $CH_4$ flux by about 20–90% (Frenzel 2000). Only ebullition of $CH_4$ seems to be not attenuated by methanotrophic activity.

Formation of gas bubbles in methanogenic soil layers is a common feature. In unvegetated rice field soil, for example, bubbles are frequently found at depth $> 10$ mm below the soil surface (Rothfuss and Conrad 1998). However, little is known about the relationship between production rates of $CH_4$ and other gases, gas flux to the atmosphere, vertical concentration profiles of dissolved gases and the zonation of formation and breakdown of gas bubbles. Martens et al. (1998) reported a kinetic model for organic-rich marine sediments dominated by sulfate reduction, methane production and methane oxidation. More recently, Bazhin (2001) published a model of gas transport in unvegetated freshwater sediments that is based on first-principle theory and allows the prediction of gas bubble flux from $CH_4$ production rates or depth of bubble formation. An extension of the model (Bazhin 2003) allows the prediction of gas bubble flux from the stationary concentrations of $CH_4$ and $N_2$ in the deep soil.

Our study intended to test the model [in particular the first part described in Bazhin (2001)] by experiments using microcosms of flooded rice field soil. Although the model is based on first principles that do not need to be tested anymore, it has not yet been applied to an environmental system, in which all relevant parameters are measured, including gas concentrations, production rates and upper boundary of bubble formation. The confrontation of the model with experimental data may illustrate possible problems in the experimental and/or computational determination of model parameters. The microcosms of flooded rice field soil offered idealized conditions, in particular homogeneous soil and constant temperature. Individual microcosms were

incubated at different constant temperatures, under oxic and anoxic conditions. We used diffusion probes (Rothfuss and Conrad 1994) to measure vertical $CH_4$ and $CO_2$ concentration profiles in unvegetated rice field soil microcosms with a resolution of about 3 mm.

## Methods

### *The model*

The model is extensively described by Bazhin (2003, 2001). The concept is outlined in Figure 1. Atmospheric gases, mainly $N_2$ and $O_2$, diffuse into the water column and further into the soil. Henry's law gives the concentrations of these gases in the soil (dissolved state)

$$C_i = K_i P_0 X_i = K_i P_i \tag{1}$$

where $C_i$ = concentration of dissolved gas in the soil; $K_i$ = Henry's constant for the flooded soil (mole $cm^{-3}$ $bar^{-1}$); $X_i$ = mixing ratio and $P_i$ = partial pressure (bar) of the $i$th gas in the atmosphere; $P_0$ = atmospheric pressure (bar). Bubble formation can only take place when the following condition is satisfied:

$$\Sigma P_i = \Sigma C_i / K_i \geq P_0(1 + b/b_0) \tag{2}$$

$b$ = thickness of water column above the soil, normalized to the depth at which hydrostatic pressure is equal to 1 atm ($b_0$). In flooded rice soil, $O_2$ is consumed

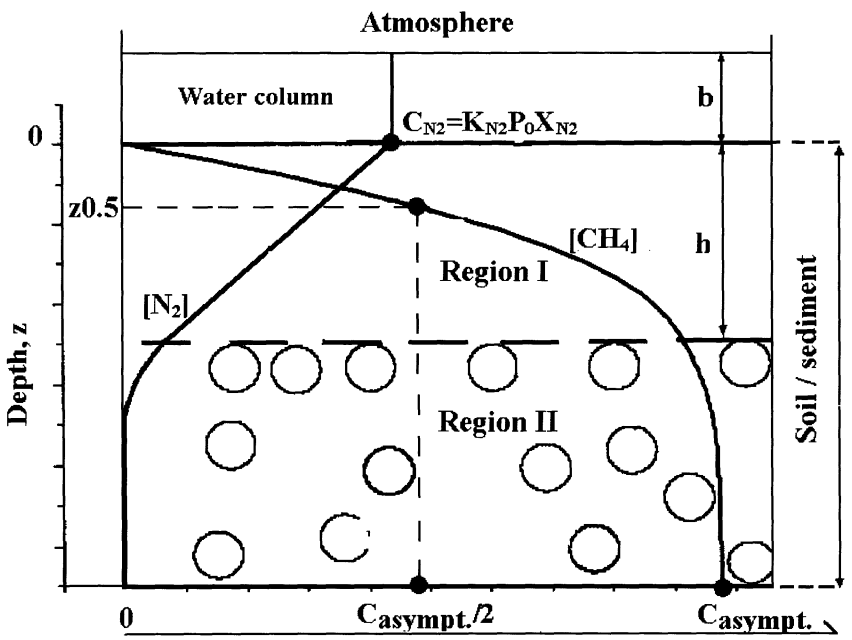


*Figure 1.* Conceptual scheme of the structure of flooded soil/sediment [adapted from (Bazhin 2001)].

within the upper 2–3 mm soil layer (Frenzel et al. 1992). In Region I, all $CH_4$ and $CO_2$ produced leave the soil by molecular diffusion, their concentrations rise with depth, but still are not sufficient to satisfy the condition of bubble formation. Condition (2) will be satisfied in Region II, with $h$ being the upper boundary of bubble formation. For a flooded soil, $x$ is the thickness of the upper oxic layer ($x < h$), where only aerobic formation of $CO_2$ takes place, with a production rate $W_{CO_2-ox}$ (mol $cm^{-3}$ $s^{-1}$). Below the oxic layer, $CH_4$ and $CO_2$ are produced with rates $W_{CH_4}$ and $W_{CO_2}$, respectively. If $W_i$, $K_i$ and diffusion coefficients ($D_i$) are constant with depth, the Equation 8 in Bazhin (2001) is reduced to:

$$h = \sqrt{\frac{2P_0(1 - X_{N_2}) + \frac{x^2 W_{CH_4}}{K_{CH_4} D_{CH_4}} + \frac{x^2 \left(W_{CO_2} - W_{CO_2-ox}\right)}{K_{CO_2} D_{CO_2}}}{W_{CH_4}/K_{CH_4} D_{CH_4} + W_{CO_2}/K_{CO_2} D_{CO_2}}} \tag{3}$$

Usually we can neglect the shallow oxic surface layer (i.e. $x = 0$), thus $h$ is given by (according to Equation 11 in Bazhin (2001)):

$$h = \sqrt{\frac{2P_0(1 - X_{N_2})}{\frac{W_{CH_4}}{K_{CH_4} D_{CH_4}} + \frac{W_{CO_2}}{K_{CO_2} D_{CO_2}}}} \tag{4}$$

If $X_{N_2}$ approaches unity (or, alternatively, production rates become high), $h$ approaches zero.

In oxically incubated microcosms, $CH_4$ and $CO_2$ concentrations in region I are described by Equations (5a) and (5b), respectively, with $A_i = dC_i(z)/dz$ at $z = 0$:

$$C_{CH_4}(z) = (-W_{CH_4}/(2D_{CH_4}))z^2 + A_{CH_4} z + C_{CH_4}(z = 0) \tag{5a}$$

$$C_{CO_2}(z) = (-W_{CO_2}/(2D_{CO_2}))z^2 + A_{CO_2} z + C_{CO_2}(z = 0) \tag{5b}$$

Note that $A_i$ can be used to calculate the diffusive flux of the $i$th gas.

For region II, bubble formation has to be taken into account, so that $CH_4$ concentration is described by:

$$C_{CH_4}(z) = B \exp(-\gamma z) + K_{CH_4} P_0 \tag{6}$$

The coefficients $\gamma$, $B$ and $A$ are given by (for details see Bazhin (2001)):

$$\gamma = \sqrt{W_{CH_4}/K_{N_2} D_{N_2} P_0 (1 + b/10)} \tag{7}$$

$$B = \left[\frac{h^2 W_{CH_4}}{2D_{CH_4}} - K_{CH_4} P_0 + C_{CH_4}(z = 0)\right]\left(\frac{\exp \gamma h)}{1 + \gamma h}\right) \tag{8}$$

$$A_{CH_4} = \frac{h W_{CH_4}}{D_{CH_4}} - \left[\frac{h^2 W_{CH_4}}{2D_{CH_4}} - K_{CH_4} P_0 + C_{CH_4}(z = 0)\right]\left(\frac{\gamma}{1 + \gamma h}\right) \tag{9}$$

Coefficient $\gamma$ reflects the vertical tendency of $CH_4$ concentration in the Region II towards saturation. In contrast to $A_{CH_4}$ and $B$, $\gamma$ does not depend on the presence of oxygen. In anoxically incubated microcosms, region I does not exist, so that the concentration gradient of $CH_4$ at the soil surface is given by:

$$dC_{CH_4}/dz(z = 0) = -B\gamma. \tag{10}$$

The $CO_2$ concentration is well described by (5b), since $CO_2$ usually contributes only about 3–4% to bubble formation (Chanton et al. 1989).

If $W_{CH_4}$ is constant with depth, the model (Bazhin 2003) predicts that $N_2$ concentrations should become zero and $CH_4$ concentrations should reach saturation at a certain depth. This depth is given by $z = (3 \text{ to } 5)\, l$, with $l$ being the characteristic length. The characteristic length is defined by

$$l = \sqrt{K_{CH_4} D_{CH_4} / W_{CH_4}} \tag{11}$$

The model of Bazhin (2001, 2003) was used to mutually calculate $W_{CH_4}$, $J_{CH_4\text{-dif}}$ and $h$ when one of these parameters has been determined experimentally (Calculated parameters are indicated by superscript 'calc', those experimentally determined by 'exp'). Thus, knowing $W^{exp}_{CH_4}$, $J^{calc}_{CH_4\text{-dif}}$ is obtained by the following algorithms for oxic and anoxic microcosms, respectively: For anoxic soils $W^{exp}_{CH_4}$ allows finding $\gamma^{calc}$ using Equation (7); coefficient $B$ is found from Equation (8), assuming $h = 0$. We find $A_{CH_4}$ from the Equation (9) and subsequently compute $J^{calc}_{CH_4(dif)}$ from the following equation:

$$J^{calc}_{CH_4(dif)} = A_{CH_4} D_{CH_4} \tag{12}$$

Knowing $h^{exp}$ in oxic soils (in anoxic soils $h$ is close to zero), $W^{calc}_{CH_4}$ can be computed from Equation (4). Then, using $W^{calc}_{CH_4}$, $\gamma^{calc}$ is computed from the Equation (7), $A_{CH_4}$ from Equation (9), and finally $J^{calc}_{CH_4\text{-dif}}$ from $A_{CH_4}$ and Equation (12).

Knowing $J^{exp}_{CH_4\text{-dif}}$, we can compute $A_{CH_4}$ from Equation (12). Coefficient $B$ is found from Equation (8), assuming $h = 0$. Then, $\gamma^{calc}$ is computed from Equation (10), and finally $W^{calc}_{CH_4}$ from Equation (7). For oxic microcosms, $W^{calc}_{CH_4}$ and $h^{exp}$ can be computed as well, but equations must be solved numerically.

The model of Bazhin (2001, 2003) was also used to calculate $W_{CH_4}$, $J_{CH_4\text{-dif}}$ and $h$ by fitting the vertical $CH_4$ concentration profiles measured in the various microcosms either to the logarithmic form (designated LOG, only used for Region II) of Equation (6):

$$\ln(K_{CH_4} P_0 - C_{CH_4}(z)) = \ln(B) - \gamma z \tag{13}$$

or to the linear form (designated LIN, only for data points in the upper 1–2-cm soil layer) of the Equation (5):

$$(C(z) - C(z = 0))/z = B_2 z + B_1 \tag{14}$$

Fit of the Equation (13) gives the input parameter $\gamma^{exp}$. Then, both for oxic and anoxic soils $W^{calc}_{CH_4}$ can be directly computed using Equation (7). $J^{calc}_{CH_4\text{-dif}}$ is then computed from $W^{calc}_{CH_4}$ as described above. Fit of the Equation (14) both in oxic and anoxic soils yields parameter $B_2$. Since

$$B_2 = -W_{CH_4}/(2D_{CH_4}) \tag{15}$$

$W^{calc}_{CH_4}$ can be computed. Parameter $B_1$ is equal to $A_{CH_4}$, so that $J^{calc}_{CH_4\text{-dif}}$ can be computed using Equation (12).

Concerning application of the model to $CO_2$, Equation (14) was fitted to $CO_2$ concentration data over the whole profile depth. $B_1$ allows then to compute $J^{calc}_{CO_2(dif)}$ and $B_2$ to compute $W_{CO_2}$. Note, that if we neglect $CO_2$ in gas bubbles, $J_{CO_2(dif)}$ is directly related to the $W_{CO_2}$. We neglected $CO_2$ in gas bubbles, thus $J_{CO_2(dif)}$ could be directly related to $W_{CO_2}$.

*Soil incubation*

The paddy soil was sampled from Italian rice fields during winter time and was stored as described by Mayer and Conrad (1990). The soil (fresh soil) was used for growing rice in our greenhouse. After harvest, this soil (recycled soil) was air-dried, sieved (1 mm mesh size) and filled into glass beakers for oxic incubation and into Plexiglas® containers for anoxic incubation (Figure 2). The soil in these microcosms was then flooded with demineralized water, mixed to avoid entrapment of air bubbles and to ensure homogenous porosity. To check model predictions more thoroughly, we modified gas production rates in some microcosms by either addition of pieces of rice straw (20 mg dry straw per gram dry soil) or mixing of soil with quartz sand (1 part soil + 4 parts quartz). We

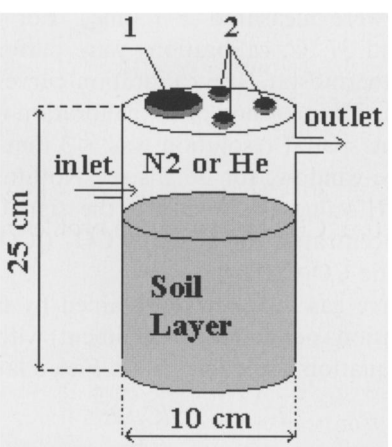


*Figure 2.* Schematic design of the microcosm for anoxic incubations. Opening 1 was used to fill microcosm with soil, openings 2 served as hatchways in measurements with a probe.

also prepared microcosms with multi-layer profiles by alternatively filling the vessels with soil/quartz sand/soil or with fresh soil/recycled soil. Experimental conditions and dimensions of all soil layers are given in Table 1. The microcosms were then incubated at constant temperature (4, 25, 37 °C) under ambient air (oxic incubations) or after flushing under $N_2$ or He (anoxic incubations). After 3–9 months of incubation (Table 1), when steady state conditions ($W_{CH_4} = W_{CO_2}$) were presumably reached (compare Yao and Conrad (2000)), we measured concentration profiles and emission rates of $CH_4$ and $CO_2$.

*Measurement of concentration profiles using gas diffusion probes*

Vertical profiles of dissolved $CH_4$ and $CO_2$ concentrations were measured using gas diffusion probes (Rothfuss and Conrad 1994; Rothfuss et al. 1994). The probes work by the following principle. The dissolved gas diffuses from the soil aqueous phase through a tiny window that is covered with a gas-permeable silicone membrane into the probe. After a certain time, the accumulated gas is flushed out with $N_2$ or He and analysed by gas chromatography. Note, that the gas sampling is finished long before equilibration is reached between the soil aqueous phase and the gas phase in the probe. The flux through the silicone membrane and consequently the analytical signal depends on the gas transport in the soil towards the membrane and thus on the porosity and tortuosity of the soil. To account for this, the probes were calibrated using an artificial sediment of glass beads (0.1 mm size) soaked with aqueous $CH_4$ or $CO_2$ standard solutions. By using this calibration method, Rothfuss and Conrad (1994) obtained a good agreement between the measured and tabulated Henry's law coefficient for $CH_4$.

The probes were calibrated using standard solutions with about 6 different $CH_4$ concentrations (0–650 $\mu$M) and $CO_2$ concentrations (0–3700 $\mu$M). All concentration points were measured 2–3 times. For measurement in soils incubated at 4, 25, and 37 °C, calibrations were performed at all respective temperatures using a thermostat. The calibration curves gave signals proportional to concentration. The precision of the calibration was about 3–5% (error of the linear slope), the spatial resolution was $< 3$ mm [considering diffusion path and size of probe-window; for details see Rothfuss et al. (1994)]. Calibration at different pH values showed that the signal of $CO_2$ was linearly dependent on the concentration of aqueous $CO_2$ ($[CO_2]_{(aq)}$) rather than on dissolved total inorganic $CO_2$($\Sigma CO_2$).

Experimental diffusive gas fluxes were obtained by fitting the gas concentration data (concentrations per volume of sediment) within the upper 0–1.5 cm soil layer to a linear equation according to 1st Fick's law:

$$J_{i(\mathrm{dif})} = D_i dC_i/dz \tag{16}$$

All data fits were performed using the computer program Origin®6.1. Henry constants and diffusion coefficients were corrected for the actual conditions in

*Table 1.* Conditions of soil incubation and experimental data.

| Index | Soil type | $T$ (°C) | Gas headspace | Incubation time, months | $N_{profiles}$ | Dimensions of microcosm (ø, cm/depth, cm) | $h$ (cm) | $W_{CH_4}$ ($10^{-12}$ mol cm$^{-3}$ s$^{-1}$) | $l$ (cm) | $J_{CH_4\text{-dif}}$ ($10^{-12}$ mol cm$^{-2}$ s$^{-1}$) | $J_{CH_4\text{-dif}}$/ $CH_4$ total flux | $\varphi_g$ |
|---|---|---|---|---|---|---|---|---|---|---|---|---|
| OX1_25 | R | 25 | Air | 3.5 | 2 | 7.06/8.4 | 1.25 ± 0.1 | 1.12 ± 0.34 | 1.8 | 1.15 ± 0.623 | 0.13 | 0.23 |
| OX2_25 | R | 25 | Air | 3.5 | 2 | 7.06/7.9 | 1.25 ± 0.1 | 1.28 ± 0.26 | 1.7 | 0.97 ± 0.55 | 0.10 | 0.24 |
| OX3_25 | R+ | 25 | Air | 4 | 3 | 7.6/9.4 | 1 ± 0.27 | 2.74 ± 0.091 | 1.2 | 1.72 ± 0.48 | 0.069 | 0.10 |
| OX4_25 | * | 25 | Air | 4 | 2 | 7.6/11.2 | 0.9 ± 0.21 | 1.48 ± 0.64 | 1.6 | 1.4 ± 1.24 | 0.086 | 0.18 |
| OX5_25 | ** | 25 | Air | 4 | 2 | 7.6/12 | 1.1 ± 0.14 | 1.59 ± 0.10 | 1.5 | 1.73 ± 0.41 | 0.093 | 0.20 |
| OX1_37 | R | 37 | Air | 2.5 | 2 | 7.6/11.5 | 0.9 ± 0.26 | 1.35 ± 1.13 | 1.7 | 2.75 ± 0.33 | 0.18 | 0.25 |
| OX2_37 | R | 37 | Air | 2.5 | 2 | 7.6/11.5 | 0.7 ± 0.1 | 1.88 ± 0.084 | 1.4 | 0.885 ± 0.97 | 0.041 | 0.25 |
| AN1 | R+ | 24 | N2 100% | 4 | 3 | 10/14.5 | ~0.2 | 2.1 ± 0.46 (SL) | 1.3 | 3.43 ± 0.97 | 0.11 | 0.20 |
| AN2 | R+ | 24 | N2 100% | 5 | 3 | 10/13.9 | ~0.2 | 1.9 ± 0.67 (SL) | 1.4 | 3.00 ± 0.29 | 0.11 | 0.20 |
| AN3 | R | 24 | N2 100% | 5 | 1 | 11.1/13.2 | ~0.2 | 0.93 ± 0.52 | 2.0 | 1.23 ± 0.23 | 0.10 | n.d. |
| AN4 | R | 24 | He 100% | 5 | 2 | 10/14.5 | ~0.2 | 1.29 ± 0.22 | 1.7 | 1.29 ± 0.29 | 0.07 | n.d. |
| Soils with low $CH_4$ and $CO_2$ production | | | | | | | | | | | | |
| OX6_25 | M | 25 | Air | 9 | 2 | 9.9/10.7 | 1.5 ± 0.13 | 0.144 ± 0.011 (SL) | 3.5 | 0.092 ± 0.028 | 0.069 | 0.20 |
| OX7_25 | M | 25 | Air | 6.5 | 2 | 7.06/8.05 | 1.8 ± 0.1 | 0.170 ± 0.043 | 3.2 | 0.15 ± 0.022 | 0.11 | 0.29 |
| OX1_4 | F | 4 | Air | 6.5 | 2 | 7.6/11.2 | 3.5 ± 0.2 | 0.107 ± 0.003 | 5.4 | 0.31 ± 0.227 | 0.28 | 0.08 |
| OX2_4 | F | 4 | Air | 6.5 | 2 | 7.6/10.2 | 3.7 ± 0.2 | 0.097 ± 0.010 | 5.6 | 0.24 ± 0.033 | 0.26 | 0.15 |

R – recycled soil; R+ – recycled soil with rice straw added; F – fresh soil; M – mix of recycled soil and quartz sand, 1:4; * – From the top to the bottom: 250 g recycled soil then 150 g quartz sand then 150 g recycled soil ** – From the top to the bottom: 250 g fresh soil, then 350 g recycled soil. Data on $W_{CH_4}$ marked by '(SL)' were obtained from measurements in slurry, all other from emission measurements, n.d. means that value of a parameter was not determined. $N_{profiles}$ = number of concentration profiles measured with probe.

flooded soil using Equations (18) and (19), respectively. All results are givens as mean values ± 1SD. After measurement of a vertical profile, microcosms were left undisturbed for 1–2 months before measurement was repeated. Calculation of parameters was done for each individual profile and subsequently averaged for the number of replicates indicated in Table 1.

*Measurement of concentration profiles using peepers*

We also applied a membrane equilibration pore water sampler, so-called peeper (Hesslein 1976), to check the reliability of the concentration measurements with the gas diffusion probe. The frame and the equilibration cells of the peeper used for measurement of dissolved $CH_4$ and $CO_2$ had the dimensions $15\times2\times1.5$ cm, and $0.4\times0.2\times0.8$ cm, respectively. A total of 30 equilibration cells at 0.2-cm depth intervals were filled with distilled water and covered with a 50-$\mu$m thick teflon membrane (Thomafoil-PTFE-Folie, Reichelt Chemietechnik). The peeper was inserted into the flooded soil and equilibrated for 3 months, i.e. sufficient time for complete equilibration of the water in the equilibration cells with the soil pore water. After removal of the peeper, aliquots (75 $\mu$l) of the water in each cell were sampled with a syringe and injected into small glass flasks (V = 1.8 ml) filled with pure $N_2$ (or He, when $N_2$ was measured). After equilibration of the gas and liquid phase by heavy shaking, gas samples (0.5 ml) were taken from the headspace of these flasks and analysed by gas chromatography. The measured $CH_4$ and $CO_2$ mixing ratios were used to calculate the concentrations of the gases dissolved in the soil pore water. To test for gas loss during sampling, the peeper was placed into aqueous solutions with known concentrations of $CH_4$ and $CO_2$ and waited at least 2 weeks for complete equilibration. The results showed that diffusive loss of gases during the time of processing of all peeper-cells could be neglected. Note that extraction was done using a large ratio of gas to liquid. It can be shown by theoretical calculation that this large ratio resulted in almost complete (99%) extraction of not only dissolved $CO_2$ but also of $CO_2$ produced from bicarbonate.

Peepers for $N_2$ measurements were bigger (frame: $36\times2\times4$ cm; cells: $1\times2.5\times1$ cm, at 0.5-cm depth intervals). The relatively low spatial resolution had to be tolerated, since the sensitivity of gas chromatography for $N_2$ was lower than for $CH_4$ and $CO_2$.

*Porosity determination and relevance*

In the model (Bazhin 2001) concentrations, gas production rates, Henry's constants and diffusion coefficients all refer to 1 $cm^3$ of flooded soil. Appropriate corrections require knowledge of water-filled and gas-filled porosities. Water-filled porosity ($\varphi_w$) was experimentally determined for every microcosm from the equation:

$$\varphi_w = \Delta M / V_{flooded} \quad (17a)$$

where $V_{flooded}$ = total volume ($cm^3$) of flooded soil in the vessel; $\Delta M$ = weight loss (g) after drying at 105 °C (assuming water density is 1.00 g $cm^{-3}$). Air-filled porosity ($\varphi_g$) is given by:

$$\varphi_g = V_{bubbles} / V_{flooded} \quad (17b)$$

where $V_{bubbles}$ = total volume of bubbles in flooded soil.

In the region I of flooded soil, there are no bubbles, and therefore $\varphi_g = 0$. If the soil does not contain gas bubbles at all, such as immediately after flooding, $\varphi_w$ determined by (17a) is equal to the water-filled porosity in the Region I (designated $\varphi_w^I$). For our microcosms immediately after flooding we obtained $\varphi_w^I = 0.54$, similarly as in our previous work (Rothfuss and Conrad 1994). For mixtures of quartz sand with soil, 4:1, we obtained $\varphi_w^I = 0.42$. These values apply only to Region I, but not to the entire flooded soil. When gas bubbles have been formed, the actually determined porosity $\varphi_w$ in Equation (17a) is no longer equal to $\varphi_w^I (= 0.54)$, but smaller (simply since the volume of flooded soil has increased due to bubble formation). We then used the experimental value of $\varphi_w$ and combined Equations (17a) and (17b) for determination of $\varphi_g$:

$$\varphi_g = 1 - \varphi_w / \varphi_w^I \quad (17c)$$

Because gas concentrations in the model are expressed in mole per $cm^3$ of flooded soil, the Henry constants ($K_i$) (Medard 1976) must be in mole $bar^{-1}$ $cm^{-3}$ of flooded soil (see Equation (1)), thus:

$$K_{soil} = K_{water} \varphi_w (1 - \varphi_g) \quad (18)$$

Diffusion coefficients ($D_i$) in pure water (Lerman 1979; Lide 1999) were corrected for the actual conditions in flooded soil using:

$$D_{soil} = D_{water} \varphi_w^2 / (1 - \varphi_g)^2 \quad (19)$$

The approximation $D_{soil} = D_{water} \varphi_w^2$ was validated for bubble-free rice filed soil by Rothfuss and Conrad (1994). For correction of gas-filled porosity, we assumed that the diffusion path per unit time increased by factor $1/(1 - \varphi_g)$.

*Measurement of gas production rates*

Production rates of $CH_4$ and $CO_2$ were determined by emission measurements using the closed chamber method. In anoxically incubated microcosms, $CH_4$ oxidation was not possible and the $CH_4$ emission rate was therefore assumed to be equal to the $CH_4$ production rate. Emission rates were determined by closing the inlet and outlet of the microcosms (Figure 1) and measuring the temporal increase of the $CH_4$ mixing ratio in gas headspace. In oxically incubated microcosms, $CH_4$ oxidation was inhibited (see below). Conse-

quently, $CH_4$ emission rates were assumed to be equal to $CH_4$ production rates. A glass beaker with the soil was placed into a Plexiglas® chamber (height: 20 cm, Ø: 11 cm) and $CH_3F$ (12–16 ml) was injected into the headspace (giving 1–1.5% $CH_3F$ by volume) to inhibit methanothrophic activity (Oremland and Culbertson 1992; Bosse and Frenzel 1998). During the following 2–3 days, gas samples (0.5 ml) were repeatedly taken from the headspace and analysed by gas chromatography. The temporal increase of $CH_4$ and $CO_2$ in the headspace was linear ($R > 0.90$, $p < 0.05$). Emission rates ($E$) were calculated by linear regression and expressed per time and microcosm.

In some soils (indicated in Table 1), production rates were measured using soil slurries (Popp et al. 2000). A soil core (Ø = 2.6 or 4.6 cm) was taken and cut into 2–10-mm slices. The slices were transferred to 75-ml bottles and diluted with 10 ml anoxic sterile water. Bottles were closed, flushed with $N_2$ and incubated in the dark at the temperature indicated in Table 1. Production rates in slurries ($P_{dry}$) were calculated using linear regression of gas concentrations vs. time and expressed per dry weight of soil ($m_{dry}$) after drying at 105 °C for 2 days. These rates (mole $g^{-1}$ $s^{-1}$) were then transformed to rates per volume ($V_{bubble\text{-}free}$) of bubble-free flooded soil, denoted $W_{CH_4}$ and $W_{CO_2}$ (mole $cm^{-3}$ $s^{-1}$) using:

$$W = m_{dry} P_{dry} / V_{bubble-free} \tag{20}$$

alternatively, from gas emission rates, using:

$$W = E / V_{bubble-free} \tag{21}$$

Knowing $V_{flooded}$, $h$ and $\varphi_g$ we obtain:

$$V_{bubble-free} = (V_{flooded} - hS)(1 - \varphi_g) + hS = V_{flooded}(1 - \varphi_g) + hS\varphi_g \tag{22}$$

where $S$ = surface area of the microcosm. Note that production rates determined in this way refer to Region I of the soil. Production rates for Region II were obtained from Equation (23) accounting for the soil volume occupied by bubbles being not active in gas production:

$$W^{II} = W(1 - \varphi_g) \tag{23}$$

(we assumed no change of the methanogenic activity per active volume in the soil near the bubbles).

Note that the error (coefficient of variation) in determination of $P_{dry}$ and $V_{bubble-free}$ was only a few percent, of $m_{dry}$ even less. However, production rates derived from the $CH_4$ emission rates in the presence of the methanotrophic inhibitor $CH_3F$ are likely to have an uncertainty of a least 10%.

The ratio of $W_{CO_2\text{-}ox}/W_{CO_2}$ (required for utilization of Equation 3, also see Section '*Experiments using different $N_2$:$O_2$ ratio in the gas headspace*') was estimated from emission measurements in OX1_25 and OX2_25. $E_{CO_2}$ was generally larger than $E_{CH_4}$ even when $CH_4$ oxidation was inhibited. Apparently, additional $CO_2$ was produced in the upper oxidized soil layers where $CH_4$ production was not taking place. Therefore, we assumed that the total $CO_2$

production consisted of $CO_2$ produced in the anoxic and in the oxic zone. Since $W_{CO_2\text{-anox}} = W_{CH_4}$, as found for anoxic microcosms, we calculated $W_{CO_2\text{-ox}}$ = [(emission rate of $CO_2$ – emission rate of $CH_4$)/volume of oxic layer].

*Experiments using different $N_2$:$O_2$ ratio in the gas headspace*

Rice soil (~20 g, the same as used for OX1_25,OX2_25) was filled into glass pressure tubes (length = 25 cm, $V$ = 26 ml), flooded with distilled water, mixed, closed with rubber stoppers and incubated under 25 °C. The gas headspace was regularly flushed with one of the following gas mixtures: 100% $O_2$; 75% $O_2$ in $N_2$; 50% $O_2$ in $N_2$; and ambient air. After 1.5 month, the upper bubble boundary $h$ was measured. To check for agreement of the measured $h$ with that determined by model equation (see below), values of $x$ (thickness of upper oxic layer) and of production rates ($W$) were required. The latter ($W_{CH_4} = W_{CO_2}$) were measured using soil slurry (Equation (20)). Then, from $W_{CO_2}$ and the ratio $W_{CO_2\text{-ox}}/W_{CO_2}$, $W_{CO_2\text{-ox}}$ was determined. Values of $x$ were supposed to be equal to the thickness of the upper brownish soil layer (caused by Fe(III) ions), or were calculated from Fick's law and the $O_2$ partial pressure assuming zero-order kinetics for bacteria oxidizing organic matter.

*Analytical techniques*

$CH_4$ and $CO_2$ were analysed by gas chromatography using a flame ionisation detector (Shimadzu). The column (Haysep D, 80/100, 3 m; 1/8″) and detector temperature were 40 °C and 120 °C respectively. The carrier gas was hydrogen. $CO_2$ was measured after conversion to $CH_4$ in a methanizer (Ni catalyst at 350 °C; Chrompack). $N_2$ was analysed with a thermal conductivity detector (Shimadzu). The column (2 m) was filled with molecular sieve 5 Å, 80/100, the operation temperature was 80 °C, the carrier gas was helium. Samples were injected using pressure-lock syringes (Precision Sampling Corp., Baton Rouge, USA).

Vertical profiles of pH in the soil microcosms were measured using a glass microelectrode (Orion combination micro pH electrode, needle tip diameter = 2 mm). Dissociation constants for $CO_2$-bicarbonate system at different temperatures were taken from Weast (1977).

The upper boundary of bubble formation, $h$, was determined visually.

## Results

*Experimental data*

The designations and major experimental conditions for the various soil microcosms are listed in Table 1. The experimental data are means ± SD of several replicates.

*Data from gas production rates*

The visible upper boundary ($h$) of the bubble layer was determined repeatedly during the incubation time ($n > 5$). It ranged between 8 and 37 mm depth (Table 1). In the anoxic microcosms (AN1–AN4) it was generally $< 2$ mm depth, demonstrating that bubble formation occurred up to the soils surface.

Production rates ($W_{CH_4}$) were from 5 or 3 replicates when measured in slurry or from emission, respectively. In most cases production rates of $CH_4$ ($W_{CH_4}$) and $CO_2$ ($W_{CO_2}$) were obtained from emission measurements. In anoxic microcosms that had reached stationary conditions, $W_{CO_2}$ was equal to $W_{CH_4}$ as expected theoretically (Yao and Conrad 2000). In oxic microcosms, $W_{CH_4}$ was obtained from the $CH_4$ emission in the presence of $CH_3F$ as inhibitor of $CH_4$ oxidation. At room temperature and 37 °C, values of $W_{CH_4}$ were similar in oxically and anoxically incubated soil microcosms (Table 1). Microcosms with mixtures of soil and quartz sand (OX6_25, OX7_25) and microcosms incubated at 4 °C (OX1_4, OX2_4) exhibited much lower values of $W_{CH_4}$.

The characteristic length ($l$) is directly related to $W_{CH_4}$ through Equation (11). This value is useful for scaling (see below) and indicates whether the vertical $CH_4$ concentration profile in this particular microcosm can be expected to reach the asymptotic value (maximum $CH_4$ concentration) within the total depth of the microcosm. In homogenous quartz/soil mixtures (OX6_25, OX7_25) and soils incubated at 4 °C (OX1_4, OX2_4), $l$ was relatively large ($> 3.5$ and $> 5$ cm, respectively) due to low $CH_4$ production rates. In these soils, maximum $CH_4$ concentrations were not reached.

Gas-filled porosity ($\varphi_g$) was determined as average for the entire soil microcosms that were incubated anoxically, or for region II in the oxically incubated microcosms. Gas-filled porosity was due to $CH_4$ production and formation of gas bubbles. Values of $\varphi_g$ ranged between 0.1 and 0.25 (Table 1), the error being about $\pm 0.01$.

*Data from vertical gas concentration profiles*

Peepers were installed in soil microcosm OX6_25. Vertical concentration profiles of $CH_4$ and $CO_2$ were measured first by using the gas diffusion probe, and then by analysing the water samples in the peeper. The results for the $CH_4$ concentrations are shown in Figure 3. In general $CH_4$ concentrations increased with soil depth. Some data points measured with the gas diffusion probe were dramatically higher than those measured with the peeper. This difference was probably caused by the presence of $CH_4$ gas bubbles near the tip of the diffusion probe, which is known to increase the signal of the probe dramatically (Rothfuss et al. 1996; Rothfuss and Conrad 1998). Indeed, using a soil (not listed in Table 1), which was incubated at 15 °C and where $CH_4$ concentrations were low and no bubbles occurred due to low production rates, the $CH_4$ profiles obtained by the two methods agreed much better (Figure 3b).

However, the $CO_2$ concentrations measured with the gas diffusion probe were systematically lower than those measured with the peeper (data not shown). This difference can be explained by assuming that the latter method

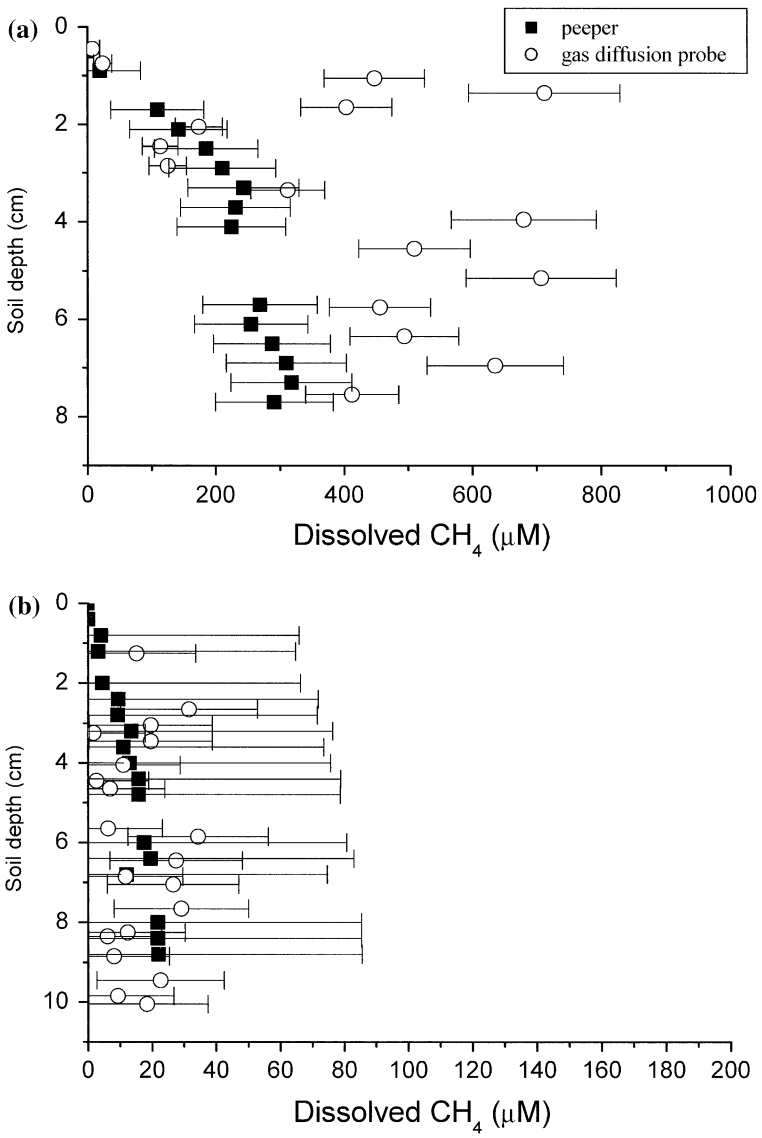


*Figure 3.* Vertical concentration profiles of $CH_4$ measured by using a peeper (closed squares) and a gas diffusion probe (open circles) in two different microcosms (a) OX6_25 and (b) a microcosm with recycled soil incubated at 15 °C. Single measurements; error bars give SD of calibration.

measured total inorganic $CO_2$($\Sigma CO_2$), while the former measured (see Methods) only dissolved $CO_2$ gas ($[CO_2]_{aq}$). Calculation of $\Sigma CO_2$ from $[CO_2]_{aq}$ using $\Sigma CO_2 = [CO_2]_{aq}(1 + K_1/[H^+])$ indeed resulted in a much better agreement of the two data sets. Hence, we assume that the $CO_2$ data obtained with the

gas diffusion probe represent dissolved concentrations of $CO_2$ gas relatively well.

Measurements of $N_2$ concentration profiles were determined by the peeper technique in a microcosm incubated at 25 °C under air (not shown in Table 1). Small $O_2$ concentrations that were usually also detected, were considered as air contamination during sampling of water from the peeper-cells. To correct for this contamination, we assumed contamination by atmospheric $N_2$ being proportional to $O_2$ contamination, and subtracted this amount from the measured $N_2$ concentration. After correction, the $N_2$ concentrations exhibited a relatively large error (Figure 4). Nevertheless, $N_2$ concentrations showed a tendency to decrease with soil depth, starting at a value corresponding to the atmospheric $N_2$ ratio (~460 $\mu$M $N_2$) down to about ~50 $\mu$M $N_2$. According to Bazhin's model (Bazhin 2001, 2003), $N_2$ concentrations should asymptotically reach zero, if gas production rates ($W_{CH_4}, W_{CO_2}$) are independent of soil depth. The $N_2$ concentration data indeed agreed fairly well with this model assumption.

From the concentration profiles in the different microcosms we estimated the asymptotic concentrations of $CH_4$ and $CO_2$ by averaging ≥5 data points within several centimetres from the bottom. The asymptotic gas concentrations were converted into the corresponding gas partial pressures ($P_{CH_4}; P_{CO_2}$) using Henry's law. Assuming that total pressure ($P_0$) is balanced by dissolved $N_2$, we obtained the partial pressure of $N_2$ by $P_{N_2} = P_0 - P_{CH_4} - P_{CO_2}$. Results

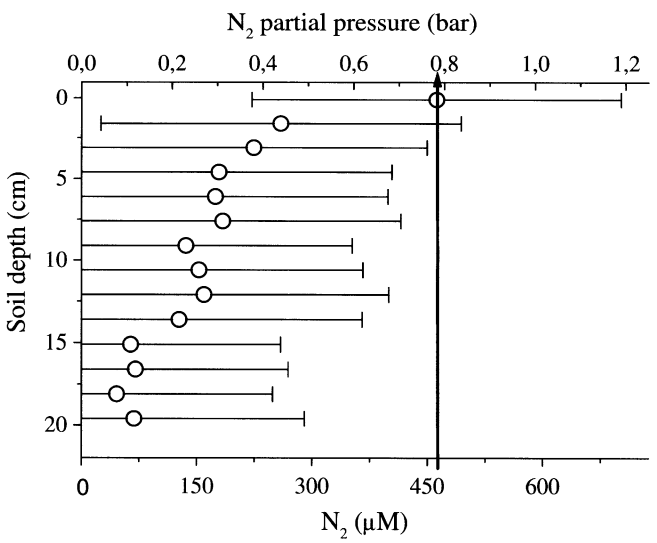


*Figure 4.* Vertical $N_2$ concentration profiles measurements in soil microcosms consisting of recycled soil incubated oxically at 25 °C. Error bars give the net error originating from calibration of the peeper and from analysis by gas chromatography. The vertical line shows the $N_2$ concentration corresponding to the atmospheric mixing ratio.

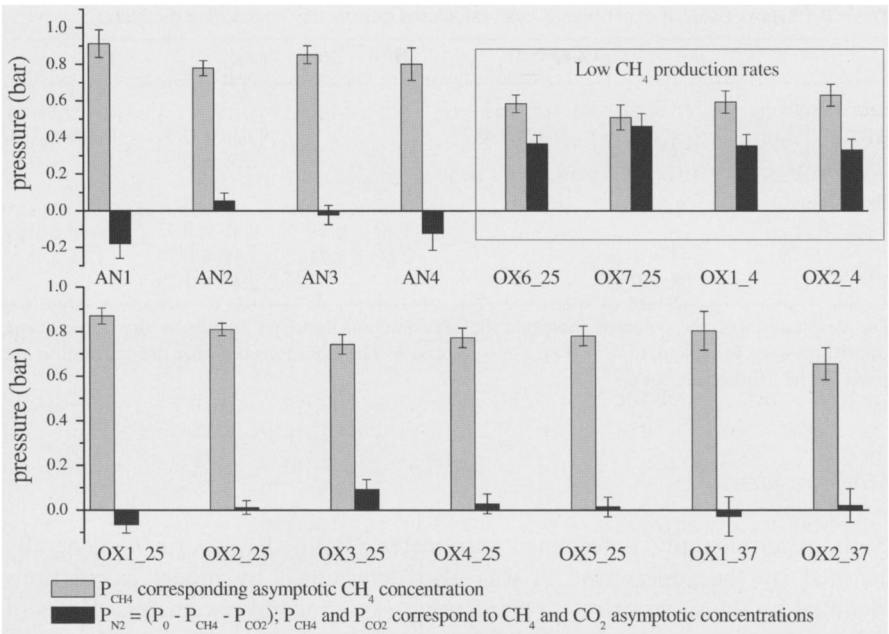


*Figure 5.* Asymptotic $CH_4$ and $N_2$ partial pressures in different soil microcosms. The average ± SD over concentration profiles (number of replicates see Table 1) is shown for each microcosm.

obtained from the different soil microcosms are shown in Figure 5. In the anoxic soil microcosms, $CH_4$ partial pressures were around 0.9 bar and thus close to the theoretical asymptotic value of $P_0$ (Equation 6). $P_{N_2}$ should be virtually zero in these microcosms. In most oxic soil microcosms incubated at 25 °C, and 37 °C the situation was similar. By contrast, for soil/quartz mixtures (OX6_25, OX7_25) and soils incubated at 4 °C (OX1_4, OX2_4), $P_{CH_4}$ was markedly lower than 1 bar, and $P_{N_2}$ greater than zero; being in accordance with prediction from $l$ (see Discussion).

Similarly, experimental $CH_4$ diffusive fluxes ($J_{CH_4\text{-dif}}$) were determined from the vertical $CH_4$ concentration profiles using Equation (16) and are also listed in Table 1. $J_{CH_4\text{-dif}}$ was found from the linear fit on every single profile, and then averaged over the number of profiles indicated in Table 1. We also calculated ratios of diffusive to total $CH_4$ flux ($J_{CH_4\text{-dif}}/J_{CH_4}$), the latter being determined from $W_{CH_4}$, the total soil depth and the thickness ($x$) of the oxic surface layer. This ratio ranged between 0.05 and 0.28 (Table 1), indicating a strong contribution of gas ebullition to total flux in most of the microcosms. It is noteworthy that the experimental data ($h, W_{CH_4}, l, J_{CH_4\text{-dif}}$) in microcosm OX4_25, which contained a layer of inactive quartz sand, were basically not different from those in OX1_25 and OX2_25, which were homogenous (Table 1).

*Table 2.* Comparison of experimental and calculated parameters concerning methane.

| | $W^{exp}_{CH_4}$ | $J^{exp}_{CH_4\text{-dif}}$ | $h^{exp}$ | LOG | LIN |
|---|---|---|---|---|---|
| Anoxic soils | | | | | |
| $W^{calc}_{CH_4}/W^{exp}_{CH_4}$ | | 0.405 ± 0.27 | | 0.630 ± 0.30 | 0.708 ± 1.60 |
| $J^{calc}_{CH_4\text{-dif}}/J^{exp}_{CH_4\text{-dif}}$ | 1.73 ± 0.88 | | | 1.359 ± 0.54 | 1.375 ± 0.67 |
| Oxic soils | | | | | |
| $W^{calc}_{CH_4}/W^{exp}_{CH_4}$ | | | 1.17 ± 0.41 | 0.48 ± 0.43 | 0.49 ± 0.61 |
| $J^{calc}_{CH_4\text{-dif}}/J^{exp}_{CH_4\text{-dif}}$ | 2.44 ± 1.26 | | 2.66 ± 1.74 | 1.18 ± 0.74 | 1.25 ± 0.21 |
| $h^{calc}/h^{exp}$ | 1.08 ± 0.23 | | | 2.48 ± 1.23 | |

The designation of the columns indicates the experimental input parameter or the curve fitting algorithms used for calculation of $W_{CH_4}$, $J_{CH_4\text{-dif}}$ and $h$. The equations used for the calculation are given in the Methods section.

## *Model results*

Each experimentally determined parameter ($W_{CH_4}, J_{CH_4\text{-dif}}$ or $h$, generally denoted by the superscript$^{exp}$) was also determined by model calculations (denoted by the superscript$^{calc}$) using other experimental parameters. Rates of $CO_2$ production were calculated from the $CO_2$ concentration profiles using different model algorithms based on Equation 6 that were fitted to data from the entire profile or just from the top 1–2 cm depth. The calculated $W^{calc}_{CO_2}$ were usually lower than the experimental values, ratios of $W^{calc}_{CO_2}/W^{exp}_{CO_2}$ being on the order of 0.2–0.6. For the calculations we only used $[CO_2]_{aq}$. When using $\Sigma CO_2$ as obtained from in the peeper experiments, values of $W^{calc}_{CO_2}/W^{exp}_{CO_2}$ were generally higher approaching unity ($W^{calc}_{CO_2}/W^{exp}_{CO_2} = 0.94 \pm 0.26$), thus confirming the model. Neglecting the $CO_2$ content of gas bubbles apparently did not cause a bias. This is reasonable, since bubbles generally contain little $CO_2$ (Chanton et al. 1989).

The $CH_4$ data were easier to interpret than the $CO_2$ data, since dissolved $CH_4$ occurs in one molecular form only. Experimental values of $W_{CH_4}, h, J_{CH_4\text{-dif}}$ were used to mutually predict $J_{CH_4\text{-dif}}, h$ and/or $W_{CH_4}$. In addition, two different ways of curve fitting to the $CH_4$ concentration profiles were used to predict $W_{CH_4}, h, J_{CH_4\text{-dif}}$. In anoxic soils, experimental values of $h$ were $< 2$ mm (Table 1), which is close to the theoretical value of zero (Equation 4). Therefore, experimental $h$ could not be used to calculate other parameters in anoxic soil. The ratios of calculated vs. experimental parameters obtained for the different microcosms were averaged over the number of microcosms and are summarized in the rows of Table 2. Generally, the range of the ratio calculated/experimental was between 0.5 and 2.7, which is a reasonable agreement given the relative imprecision of the individual input data.

Good agreement between $W^{calc}_{CH_4}$ and $W^{exp}_{CH_4}$ was even found, when using a simplified form of Equation (4), in which $CO_2$ production is not taken into account, i.e.

$$h = \sqrt{2P_0(1 - X_{N_2})K_{CH_4}D_{CH_4}/W_{CH_4}} \quad (24)$$

Figure 6a shows a plot of $(K_{CH_4}D_{CH_4}/W_{CH_4})^{0.5}$ against $h$ using values of $W^{exp}_{CH_4}$ and $h^{exp}$ measured in the various oxic microcosms. The plot showed a good linear correlation with a slope of 1.57. This value is close to theoretical value of $[2P_0(1 - X_{N_2})]^{-05}$, which is 1.543 at $X_{N_2} = 0.78$.

Experimental values of $h$ may also be used to calculate the diffusive flux of $CH_4$ ($J_{CH_4\text{-dif}}$) in a simple way. This approach follows from the assumption that $J_{CH_4\text{-dif}}$ is equal to the total $CH_4$ produced in region I, i.e.

$$J_{CH_4\text{-dif}} \approx hW_{CH_4} \quad (25)$$

This assumption is plausible, since diffusive loss of $CH_4$ from region II is low due to small concentration gradient. Therefore, nearly all the $CH_4$ produced in region II will result in bubble formation. We checked this approach using experimental values of either $W_{CH_4}$ or $h$, and calculating the second independent parameter from Equation (24) and found that this

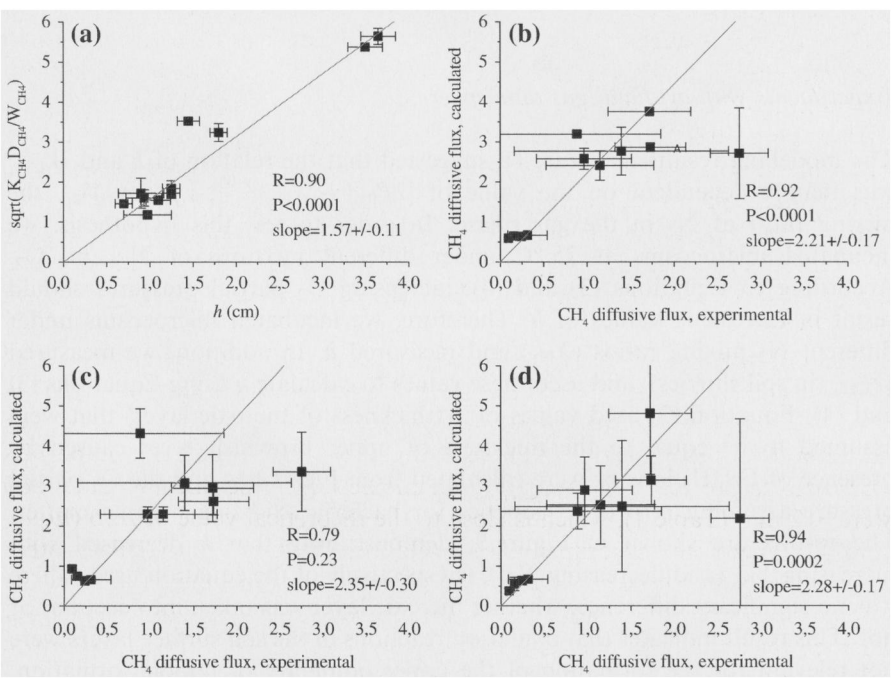


*Figure 6.* (a) Plot of $\sqrt{K_{CH_4}D_{CH_4}/W_{CH_4}}$ vs. experimental values of $h$. (b, c, d) plots of calculated vs. experimental values of $J_{CH_4\text{-dif}}$ (units in $10^{-12}$ mol cm$^{-2}$ s$^{-1}$). Experimental values of $J_{CH_4\text{-dif}}$ were obtained from gas concentration profiles fitted to Equation (16). Calculated values were from $J_{CH_4\text{-dif}} = 1.8hW_{CH_4}$, using (b) experimental $W_{CH_4}$ and $h$ from Equation (24); (c) experimental $h$ and $W_{CH_4}$ from Equation (24); (d) both experimental $W_{CH_4}$ and $h$.

simplified calculation indeed predicted values of $J_{CH_4\text{-dif}}$ relatively well ($J^{calc}_{CH_4}/J^{exp}_{CH_4} = 0.76 - 1.09$).

However, after we neglected the $CO_2$ content in the bubbles, we can also use the exact relationship between $J_{CH_4\text{-dif}}$ and $W_{CH_4}$, which is given by parameter $\tilde{a}$ (Table 1; Bazhin 2003). In particular, for production rates being constant with depth, $\tilde{a} = 1.198$ and thus

$$J_{CH_4\text{-dif}} = 1.198(K_{soil} D_{soil} W_{CH_4})^{0.5} \tag{26}$$

Combining Equation (26) with Equation (24) and using $X_{N_2} = 0.78$, and $P_0 = 1$ atm, leads to:

$$J_{CH_4\text{-dif}} \approx 1.8 h W_{CH_4} \tag{27}$$

We checked the latter approach using experimental values of either $W_{CH_4}$ (Figure 6b) or $h$ (Figure 6c), and calculating the second independent parameter from Equation (24), or just using the experimental values of both $W_{CH_4}$ and $h$ (Figure 6d). The plots in Figure 6b–d shows that this calculation overestimates values of $J_{CH_4\text{-dif}}$ relatively by a factor of about 2.2 ($J^{calc}_{CH_4}/J^{exp}_{CH_4} = 2.20 - 2.35$). Alternatively, $J^{exp}_{CH_4}$ may have been underestimated from the measured vertical concentration profiles.

*Experiments with artificial gas atmospheres*

The modelling results in Figure 6a suggested that the relation of $h$ and $W_{CH_4}$ was mainly dependent on the value of $[2P_0(1 - X_{N_2})]^{-05}$, i.e. on $X_{N_2}$, the mixing ratio of $N_2$ in the gas phase. In order to test this hypothesis, we incubated microcosms at 25 °C under different mixtures of $N_2$ and $O_2$. According to Equations (3) and (4), increasing $O_2$ partial pressures should result in increasing values of $h$. Therefore, we incubated microcosms under different $N_2$ mixing ratios ($X_{N_2}$) and measured $h$. In addition, we measured $W_{CH_4}$ (in soil slurries), and used these values to calculate $h$ using Equations (3) and (4). Equation (3) used values of $x$ (thickness of the oxic layer) that were assumed to be equal to the thickness of upper brownish layer caused by presence of Fe(III) ions or were calculated from Fick's law and the $O_2$ partial pressure assuming zero order kinetics for bacteria oxidizing organic matter. The results are shown in Figure 7, demonstrating that $h$ decreased with increasing $X_{N_2}$ (and decreasing $X_{O_2}$), irrespectively of the equation used. There was no significant difference, whether the oxic layer was taken into account or not. This result indicates that oxidation reactions in the soil surface layers were not relevant for the formation of the upper boundary of bubble formation, which under our experimental conditions was mainly caused by physical processes. A plot of ln $h$ against $\ln(1 - X_{N_2})$ (Figure 7b) resulted in a slope of $0.606 \pm 0.083$, which was close to the theoretical value of 0.5 (according to Equation (4)).

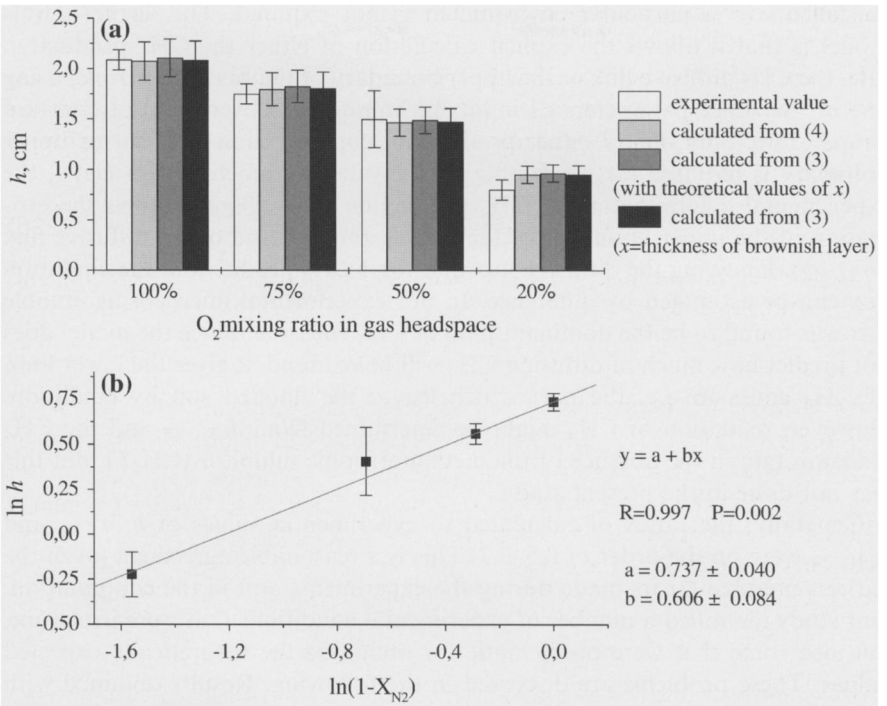


*Figure 7.* Effect of atmospheric composition on the upper boundary of the bubble zone. (a) Value of $h$ as function of the $O_2$ content of the atmosphere. (b) Plot of *ln h* (experimental value) vs. $\ln(1 - X_{N_2})$. For 100% $O_2$, $h$ is given by mean value (± SD) from four experiments, all other were means of two.

Among the anoxic microcosms, one (AN4) was incubated under He instead of $N_2$ and, subsequently $K_{He}$ and $D_{He}$ were used in Equation (7). Since $(K_{He}D_{He})/(K_{N_2}D_{N_2}) \approx 2$ (Medard 1976), coefficient $\gamma$ in Equations (6) and (13) should be affected. Namely, under a He atmosphere, $\gamma$ should be smaller than under air or $N_2$, and consequently $CH_4$ concentration should approach saturation faster under $N_2$ than He. However, the effect could not be recognized when fitting the vertical $CH_4$ concentration profiles in the different anoxic microcosms to these equations because of the rather large $W_{CH_4}$ and therefore steep $CH_4$ concentration gradients.

## Discussion

Our measurements performed with flooded soil under idealized conditions showed that the model of Bazhin (2001, 2003) is helpful for interpreting $CH_4$ concentration profiles and $CH_4$ production rates. This analytical model is based on the physical behaviour of gases dissolved in flooded methanogenic soils or sediments. Because it is based on first principles, adaptation of model

coefficients to a particular environment is not required. The virtue of this model is that it allows the explicit calculation of either the $CH_4$ production rate, the $CH_4$ diffusive flux or the upper boundary of the gas bubble zone, using one of the other parameters as input. In homogeneous sediment at constant temperature, only one of either production, concentration gradient or upper boundary is required for computing all the other parameters. Especially, the experimental determination of $CH_4$ production rates ($W_{CH_4}$) allows the estimation of the upper boundary of the bubble zone ($h$) and of the diffusive flux ($J_{CH_4\text{-dif}}$). Knowing the diffusive flux and total $CH_4$ production, the ebullition flux can be estimated by difference. In our experimental microcosms, bubble flux was found to be the dominant path of $CH_4$ emission. Since the model does not predict how much of diffusing $CH_4$ will be oxidised, it gives the lower limit of $CH_4$ emission, i.e. the part which leaves the flooded soil by ebullition. However, oxidation of $CH_4$ might be determined from $J_{CH_4\text{-dif}}$ and the $CH_4$ emission rate in the absence of the methanotrophic inhibitor ($CH_3F$), but this was not done in the present study.

Generally, the ratios of calculated to experimental values of $h$, $W_{CH_4}$ and $J_{CH_4\text{-dif}}$ were on the order of 0.5–2.7. This is a reasonable agreement given the various possible errors made during the experiments and in the computation. Our study identified a number of experimental conditions that were irrelevant, but also some that were problematic for obtaining the theoretically expected values. These problems are discussed in the following. Results obtained with soil microcosms incubated under different conditions showed that complications caused by the presence of an oxic soil surface layer could be neglected. The oxic surface layer allows increased activity of $CO_2$-producing processes. However, the model output was not very sensitive to $CO_2$, which is reasonable, since $CO_2$ is approximately 25 times more soluble than $CH_4$, and therefore does not markedly affect the position of the upper boundary of the bubble zone. On the other hand, it was sensitive to the mixing ratio of $N_2$ in the atmosphere, demonstrating the square root dependency as expected from Equation (4). Although this sensitivity should be of little practical importance (the $N_2$ mixing ratio in the atmosphere does hardly change), the general validity of Equation 4 is shown.

In our experiments, the upper boundary of the gas bubble zone ($h$) was visually determined, as described before (Rothfuss and Conrad 1998). In anoxically incubated soil, the gas bubble zone extended up to the surface. In oxically incubated soils, the value of $h$ was around 10 mm, as observed before (Rothfuss and Conrad 1998). The values increased when $CH_4$ production rates decreased, for example at low incubation temperatures (e.g. 4 °C; OX1_4, OX2_4) or usage of homogeneous mixtures of active soil and inactive quartz sand (OX6_25, OX7_25). On the other hand, values of $h$ (and of $W_{H_4}$ and $J_{CH_4\text{-diff}}$) were not affected, when a layer of inactive quartz sand was sandwiched between two layers of active soil (OX4_25). Methane production in the active layers was apparently sufficient for equilibrating the $CH_4$ concentration across the inactive layer, so that stationary $CH_4$ and $N_2$ concentrations

(Figure 5) were reached in this type of microcosm, too. Although $h$ can be easily determined in microcosm studies after long equilibration, it is not easily determined under *in-situ* conditions or in freshly sampled cores of soil and sediment. Hence, $h$ is a helpful output parameter rather than a practical input parameter for running the model.

Vertical concentration profiles of $CH_4$ and $CO_2$ were routinely measured using the gas diffusion probe described by Rothfuss et al. (1994). Alternatively, gas concentration profiles can be measured by (1) sectioning of soil cores followed by extraction; (2) application of equilibration pore water samplers (peepers; (Hesslein 1976)); (3) direct pore water sampling with micro-syringes (King 1990); (4) measurements with a membrane inlet mass spectrometer (Lloyd et al. 1996); or (5) measurement with micro-biosensor (Damgaard et al. 1998). The methods (1) and (2) are rather destructive, have only limited spatial resolution and/or require long equilibration times. Method (3) is technically problematic, because of clogging of the syringe needle with soil particles and possible damage of the gas chromatograph by direct injection. Method (4) requires special equipment, and method (5) depends on the construction of complicate biosensors with short shelf time. Therefore, we used diffusion probes for routine measurements and checked their reliability with peepers. A minor problem with gas diffusion probes is their sensitivity against the presence of gas bubbles (Rothfuss et al. 1996). Therefore, in the Region II of the soil layer, some $CH_4$ data points are outliers. Unfortunately, the $CO_2$ concentration profiles measured routinely with gas diffusion probes could not be used for model calculations without conversion to $\Sigma CO_2$. The model however, predicted $CO_2$ production rates well, when we took $\Sigma CO_2$ profile measured by peeper as input for fitting.

The vertical profiles of dissolved $CH_4$ were comparable to earlier measurements in rice field soil (Rothfuss and Conrad 1994; Rothfuss et al. 1996; Rothfuss and Conrad 1998). The model predicts an asymptotic regime of gas concentrations in region II. Indeed, concentrations of dissolved $CH_4$ became nearly constant in this region. Sensitivity of the diffusion probes against bubbles resulted in the loss of some data points in the upper part of Region II. Therefore, the fit of the concentration profile of Region II to the logarithmic equation (Equation 13) resulted in an uncertain estimation of parameter $\gamma$ and thus, poor prediction of $W_{CH_4}$. From a practical point of view it is therefore more appropriate determining $CH_4$ production rates or upper boundary of bubble formation as input parameters than measuring gas concentration profiles (see below). Alternatively, systems with low $CH_4$ production rates may be chosen, so that the $CH_4$ concentration gradients become less steep and thus easier to measure. On the other hand, these systems will require long incubation times for reaching steady state (see discussion below).

For region I (where bubbles do not interfere), on the other hand, concentration profiles were pronounced and allowed precise fitting to Equations (16) and (14), which then allowed the determination of $W_{CH_4}$ and $J_{CH_4\text{-dif}}$. In our

work, the experimental values of $J_{CH_4\text{-dif}}$ are nevertheless likely to be underestimated, since Region I was in most cases only about 1 cm thick and thus only 3–4 concentration points could be measured. Vertical concentration profiles of $CH_4$ constituted valuable input data for modelling, but increasing of spatial resolution would be helpful to improve the prediction quality by the model. Future measurements might apply instrumentation with higher precision and/or spatial resolution, e.g. microbiosensors (Damgaard et al. 1998).

From a practical perspective, determination of total gas production rates ($W_{CH_4}$) is easier than determination of vertical concentration gradients. The model allows the calculation of the upper boundary ($h$) of the gas bubble zone. Assuming that the diffusive flux $J_{CH_4\text{-dif}} = 1.8\,h W_{CH_4}$, and that the bubble flux is the difference between total flux and diffusive flux, we can calculate the bubble flux by:

$$J_{CH_4\text{-bub}} = W_{CH_4}(z - 1.8\,h) \tag{28}$$

where $z$ = depth of microcosm. The ratios of $J_{CH_4(dif)}$ to total $CH_4$ flux were in a range of 0.05–0.15, demonstrating that ebullition is the primary mechanism of methane emission innon-vegetated flooded soil.

Total $CH_4$ production was routinely measured as $CH_4$ emission flux in the presence of an inhibitor of $CH_4$ oxidation. Since the soil is homogeneous, we may assume that $CH_4$ production is constant with depth (confirmed by experiments, not shown), except for the shallow ($< 3$ mm) oxic surface layer, in which $CH_4$ production is inhibited. The depth of this zone increased with increasing $O_2$ partial pressure in the atmosphere (Figure 7c) but did not affect the determination of $W_{CH_4}$ significantly due to its small volume. In fact, however, $CH_4$ production may be suppressed in a larger volume of soil, i.e. including the upper soil layers, in which iron reduction and sulfate reduction are occurring. These processes result in production of $CO_2$ rather than $CH_4$ (Chidthaisong and Conrad 2000; Yao and Conrad 2000). The operation of these processes was seen in the higher emission rates of $CO_2$ than $CH_4$ measured in oxically incubated microcosms (data not shown). In anoxically incubated microcosms, on the other hand, emission rates of both gases were similar, as theoretically expected (Yao and Conrad 2000) and observed in numerous anoxic methanogenic environments exhibiting ratios of $CO_2$ to $CH_4$ flux around 1–1.5 (Lansdown et al. 1992; Yao and Conrad 2000). Our experimental data indicate that at 25 °C the $CO_2$ production in the upper soil layers was by a factor of 20–70 higher than $CO_2$ production in the lower anoxic layers, which is indicative for respiratory (using $O_2$, ferric iron, sulfate, etc. as oxidant) rather than methanogenic degradation of organic matter (data not shown).

Another important complication is the presence and absence of gas bubbles. By definition we have the upper region I, which does not contain gas bubbles and region II, in which gas bubbles exist. Therefore, we have to distinguish $CH_4$ production in these two zones. The $CH_4$ production rates in the two

regions, i.e. $W^{I}_{CH_4}$ and $W^{II}_{CH_4}$, can be determined if the gas-filled porosity $\varphi_g$ in region II is known, using

$$W^{II}_{CH_4}/W^{I}_{CH_4} = 1 - \varphi_g \tag{29}$$

and Equations (20) and (21) which yield $W^{I}_{CH_4}$, when using $(V_{\text{flooded soil}} - V_{\text{bubbles}})$ instead of $V_{\text{flooded soil}}$. $V_{\text{bubbles}}$ can be easily found from $\varphi_g$ and the volume of region II in the soil. Our experiments showed values of $\varphi_g$ which were in the range of 0.2–0.25, which is similar to a previous estimate (Rothfuss and Conrad 1998). They determined gas-filled porosity $\varphi_g$ in flooded rice soil microcosms, by visually determining the volume occupied by gas bubbles. At $h = 1$ cm they found $\varphi_g = 0.3$, with a decreasing tendency with depth. An important question is whether the measured $\varphi_g$ represented steady state conditions, since the dimension of region II, the total amount of bubbles and the average bubble flux will be constant, when a constant $\varphi_g$ is reached. Using the measured values of $W_{CH_4}$ it is possible to estimate the time required to reach the final $\varphi_g$. In the beginning of incubation we may assume that the volume $V$ [cm$^3$] is free of bubbles. To reach certain value of $\varphi_g$, a volume of $CH_4$ equal to $\varphi_g V/(1-\varphi_g)$ must be produced. Using $P\,V = n\,R\,T$ and assuming that bubbles are 100% $CH_4$, (which is not quite true), we calculate the amount of $CH_4$ produced as $n_{CH_4} = \varphi_g V/((1-\varphi_g)RT)$. The time required to produce this amount of $CH_4$ is then given by $t = n_{CH_4}/(VW_{CH_4})$. If we assume that $\varphi_g = 0.25$, $T = 25$ °C and $W_{CH_4} = 10^{-12}$ mol (cm$^3$ of bubble-free soil)$^{-1}$ s$^{-1}$, then steady state should be reached in 5 month. We incubated soils at least 3 months before measurements were made. This time is fairly close to the required equilibration time. Note, however, that it was much too short for incubation at 4 °C, for which equilibration time of >1 year was necessary. Therefore, $W_{CH_4}$ obtained from emission rates measured in OX1_4 and OX2_4 were most probably underestimated, since part of produced $CH_4$ stayed in Region II and increased bubble volume. Extent of underestimation is given approximately by the percentage of the theoretical bubble flux. Since $h$ was about 4 cm and $z = 10$–11 cm, then, according to Equation 28, bubble flux should have been about 30% of the total flux.

In equilibrium, $N_2$ and $CH_4$ concentrations reach their asymptotic values in region II. There are few studies on macroscale $N_2$ concentration profiles in the literature (Kipphut and Martens 1982). These data as well as our present data indeed indicate that $N_2$ concentrations decrease with depth. Assuming $W_{CH_4}$ to be constant with depth, $N_2$ concentration should be zero and $CH_4$ concentration should reach saturation at a depth that is approximately 3–5 times the characteristic length $l$ given by Equation (11) (Bazhin 2003). Values of $l$ for the different microcosms are listed in Table 1. For most microcosms l was 1.2–2.0 cm and thus at least 4 times smaller than the depth of the soil, which was 8–15 cm. In these microcosms, the calculated asymptotic $N_2$ concentration was zero (Figure 5), as predicted. By contrast, in microcosms OX1_4 and OX2_4 (4 °C) and in OX6_25 and OX7_25, $W_{CH_4}$ was low ($\sim 10^{-13}$ mole cm$^{-3}$ s$^{-1}$),

characteristic length $l$ was 3.2–5.5 cm, and the depth of microcosms was 8.5–11 cm. $P_{N_2}$ calculated for these soils was $>0.5$ bar, indicating that equilibration time was not sufficient to arrive at an asymptotic $N_2$ concentration of zero. This is due to fact that purging of $N_2$ from the deep microcosm by bubble flux needs more time if $CH_4$ production rate is low.

In conclusion, our experimental results were largely in agreement with the first part of Bazhins model (2001). The model thus allows to determine the upper boundary $h$ of the zone of bubble formation and further the ebullition flux from knowledge of either the $CH_4$ production rate ($W_{CH_4}$) or the diffusive flux ($J_{CH_4\text{-dif}}$) of $CH_4$. In particular, $CO_2$ bubble content and oxic layer thickness were confirmed to be of little relevance for model calculations. We showed that, as expected, the position of upper boundary of bubble formation does not depend on any parameter in Region II (see experiment with OX4_25). Equations (24) and (28) showed relations between $h$, $W_{CH_4}$ and $J_{CH_4\text{-bub}}$, which might be used for prediction of gas bubble flux, if values of $W_{CH_4}$ are available and these values can be reasonably applied as input over an active depth ($z$) of soil or sediment. The model may also be useful in predicting the diffusion flux of $CH_4$, which is difficult to determine by experiments unless the analytical equipment allows a high spatial resolution of the $CH_4$ concentration gradient within the surface layers. A further step would be to confirm the extension of the model (Bazhin 2003) in which a vertical decrease of the production rates is taken into account. Still further complications are caused by aquatic plants, which are considered in another extension of the model (Bazhin 2004), but have not been rigorously tested by experiments.

## Acknowledgements

We thank Peter Frenzel for numerous technical advice and useful discussion, and two anonymous reviewers for helpful criticism. The study was financially supported by the German Fonds der Chemischen Industrie. N.M. Bazhin was funded by Grant RFBR No. 04-05-64861.

## References

Bazhin N.M. 2001. Gas transport in a residual layer of a water basin. Chemosphere – Global Change Sci. 3: 33–40.

Bazhin N.M. 2003. Theoretical consideration of methane emission from sediments. Chemosphere 50: 191–200.

Bazhin N.M. 2004. Influence of plants on the methane emission from sediments. Chemosphere 54: 209–215.

Bosse U. and Frenzel P. 1998. Methane emissions from rice microcosms: the balance of production, accumulation and oxidation. Biogeochemistry 41: 199–214.

Casper P., Maberly S.C., Hall G.H. and Finlay B.J. 2000. Fluxes of methane and carbon dioxide from a small productive lake to the atmosphere. Biogeochemistry 49: 1–19.

Chanton J.P. and Dacey J.W. 1991. Effects of vegetation on methane flux, reservoirs, and carbon isotopic composition. In: Rogers J.E. and Whitman W.B. (eds), Trace Gas Emissions by Plants. Academic Press, San Diego, pp. 65–92.

Chanton J.P. and Whiting G.J. 1995. Trace gas exchange in freshwater and coastal marine environments: ebullition and transport by plants. In: Matson P.A. and Harriss R.C. (eds), Biogenic Trace Gases: Measuring Emissions from Soil and Water. Oxford, Blackwell, pp. 98–125.

Chanton J.P., Martens C.S. and Kelley C.A. 1989. Gas transport from methane-saturated, tidal freshwater and wetland sediments. Limnol.Oceanogr. 34: 807–819.

Chareonsilp N., Buddhaboon C., Promnart P., Wassmann R. and Lantin R.S. 2000. Methane emission from deepwater rice fields in Thailand. Nutr. Cycl. Agroecosyst. 58: 121–130.

Chidthaisong A. and Conrad R. 2000. Turnover of glucose and acetate coupled to reduction of nitrate, ferric iron and sulfate and to methanogenesis in anoxic rice field soil. FEMS Microbiol. Ecol. 31: 73–86.

Conrad R. 1989. Control of methane production in terrestrial ecosystems. In: Andreae M.O. and Schimel D.S. (eds), Exchange of Trace Gases between Terrestrial Ecosystems and the Atmosphere. Dahlem Konferenzen, Wiley, Chichester, pp. 39–58.

Conrad R. and Rothfuss F. 1991. Methane oxidation in the soil surface layer of a flooded rice field and the effect of ammonium. Biol. Fertil. Soils 12: 28–32.

Damgaard L.R., Revsbech N.P. and Reichardt W. 1998. Use of an oxygen-insensitive microscale biosensor for methane to measure methane concentration profiles in a rice paddy. Appl. Environ. Microbiol. 64: 864–870.

Frenzel P. 2000. Plant-associated methane oxidation in rice fields and wetlands [Review]. Adv. Microb. Ecol. 16: 85–114.

Frenzel P., Thebrath B. and Conrad R. 1990. Oxidation of methane in the oxic surface layer of a deep lake sediment (Lake Constance). FEMS Microbiol. Ecol. 73: 149–158.

Frenzel P., Rothfuss F. and Conrad R. 1992. Oxygen profiles and methane turnover in a flooded rice microcosm. Biol. Fertil. Soils 14: 84–89.

Grosse W., Armstrong J. and Armstrong W. 1996. A history of pressurised gas-flow studies in plants. Aquat. Bot. 54: 87–100.

Hesslein R.H. 1976. An *in situ* sampler for close interval pore water studies. Limnol. Oceanogr. 21: 912–914.

Keller M. and Stallard R.F. 1994. Methane emission by bubbling from Gatun Lake, Panama. J. Geophys. Res. 99: 8307–8319.

King G.M. 1990. Dynamics and controls of methane oxidation in a Danish wetland sediment. FEMS Microbiol. Ecol. 74: 309–323.

Kipphut G.W. and Martens C.S. 1982. Biogeochemical cycling in an organic-rich coastal marin basin – 3. Dissolved gas transport in methane-saturated sediments. Geochim. Cosmochim. Acta 46: 2049–2060.

Lansdown J.M., Quay P.D. and King S.L. 1992. $CH_4$ production via $CO_2$ reduction in a temperate bog: a source of $^{13}C$-depleted $CH_4$. Geochim. Cosmochim. Acta 56: 3493–3503.

Lelieveld J., Crutzen P.J. and Dentener F.J. 1998. Changing concentrations, lifetime and climate forcing of atmospheric methane. Tellus 50B: 128–150.

Lerman A. 1979. Geochemical Processes. Water and Sediment Environments. Wiley, New York.

Lide D.R. (eds) 1999. CRC Handbook of Chemistry and Physics, 80th ed. The Chemical Rubber Company, Cleveland, Ohio.

Lloyd D., Thomas K., Price D., O'Neil B., Oliver K. and Williams T.N. 1996. A membrane-inlet mass spectrometer miniprobe for the direct simultaneous measurement of multiple gas species with spatial resolution of 1 mm. J. Microbiol. Methods 25: 145–151.

Martens C.S., Albert D.B. and Alperin M.J. 1998. Biogeochemical processes controlling methane in gassy coastal sediments. 1. A model coupling organic matter flux to gas production, oxidation and transport. Cont. Shelf Res. 18: 1741–1770.

Mayer H.P. and Conrad R. 1990. Factors influencing the population of methanogenic bacteria and the initiation of methane production upon flooding of paddy soil. FEMS Microbiol. Ecol. 73: 103–112.

Medard L. 1976. Gas Encyclopaedia. Elsevier. Amsterdam.

Oremland R.S. and Culbertson C.W. 1992. Evaluation of methyl fluoride and dimethyl ether as inhibitors of aerobic methane oxidation. Appl. Environ. Microbiol. 58: 2983–2992.

Popp T.J., Chanton J.P., Whiting G.J. and Grant N. 2000. Evaluation of methane oxidation in the rhizosphere of a Carex dominated fen in north central Alberta, Canada. Biogeochemistry 51: 259–281.

Rothfuss F. and Conrad R. 1994. Development of a gas diffusion probe for the determination of methane concentrations and diffusion characteristics in flooded paddy soil. FEMS Microbiol. Ecol. 14: 307–318.

Rothfuss F. and Conrad R. 1998. Effect of gas bubbles on the diffusive flux of methane in anoxic paddy soil. Limnol. Oceanogr. 43: 1511–1518.

Rothfuss F., Frenzel P. and Conrad R. 1994. Gas diffusion probe for measurement of $CH_4$ gradients. In: Stal L.J. and Caumette P. (eds), Microbial Mats. Structure, Development and Environmental Significance. Springer, Berlin, pp. 167–172.

Rothfuss F., Bijnen F.G.C., Conrad R., Harren F.J.M. and Reuss J. 1996. Combination of photoacoustic detector with gas diffusion probes for the measurement of methane concentration gradients in submerged paddy soil. Chemosphere 33: 2487–2504.

Schütz H., Schröder P. and Rennenberg H. 1991. Role of plants in regulating the methane flux to the atmosphere. In: Sharkey T.D., Holland E.A. and Mooney H.A. (eds), Trace Gas Emissions by Plants. Academic Press, San Diego, pp. 29–63.

Wang J.S., Logan J.A., McElroy M.B., Duncan B.N., Megretskaia I.A. and Yantosca R.M. 2004. A 3-D model analysis of the slowdown and interannual variability in the methane growth rate from 1988 to 1997 [Review]. Global Biogeochem. Cycles 18: B3011-doi:10.1029/2003GB002180.

Wassmann R. 1996. Fluxes and pools of methane in wetland rice soils with varying organic inputs. Environ. Monit. Assess. 42: 163–173.

Watson R.T., Meira Filho L.G., Sanhueza E. and Janetos A. 1992. Greenhouse gases: sources and sinks. In: J.T., Callander B.A. and Varney S.K. (eds), Climate Change 1992. The Supplementary Report to the IPCC Scientific Assessment. Cambridge University Press, Cambridge, pp. 25–46.

Weast R.C. (eds) 1977. CRC Handbook of Chemistry and Physics, 58 ed. The Chemical Rubber Company, Cleveland, Ohio.

Yao H. and Conrad R. 2000. Electron balance during steady-state production of $CH_4$ and $CO_2$ in anoxic rice soil. Eur. J. Soil Sci. 51: 369–378.

Zehnder A.J.B. and Stumm W. 1988. Geochemistry and biogeochemistry of anaerobic habitats. In: Zehnder A.J.B. (ed.), Biology of Anaerobic Microorganisms. Wiley, New York, pp. 1–38.